This article has been accepted for publication in a future issue of this journal, but has not been fully edited. Content may change prior to final publication. Citation information: DOI 10.1109/JLT.2018.2877583, Journal of Lightwave Technology

A microfiber knot incorporating a tungsten disulfide saturable absorber based multi-wavelength mode-locked erbium-doped fiber laser

Shi Li, Yating Yi, Yu Yin, Yuxuan Jiang, Haiyan Zhao, Yanqiu Du, Yujin Chen, Elfed Lewis, Gerald Farrell, Sulaiman Wadi Harun, and Pengfei Wang

***Abstract*—A novel multi-wavelength mode-locked Erbium-doped fiber laser with tungsten disulfide (WS_2) combined with a microfiber knot is described. This hybrid fiber structure facilitates strong light matter interaction between the saturated absorption of the WS_2 material and high optical non-linearity of the microfiber knot. It is demonstrated experimentally that the novel fiber laser works stably in the absence of an external comb filter, with the generation of stable multi-wavelength picosecond pulses. In the multi-wavelength lasing regime, up to 7-wavelength stable mode-locked pulses are obtained using a polarization controller with the pump power at ~250 mW. The pulse period and the pulse width are 188.7 ns and 16.3 ps respectively. In addition, the number of multi-wavelength lasing channels can be changed by simply adjusting the microfiber knot size. Experimental results show the laser to have a stable output over 12 hours recording period. The results of this investigation demonstrate that the optical microfiber knot with a WS_2 overlay based fiber laser device can operate as a highly nonlinear optical component and a saturable absorber. The proposed multi-wavelength lasing device can therefore be widely used for non-linear and ultrafast photonics and has a number of advantages compared to similar devices using more conventional technologies, including low cost and good stability.**

***Index Terms*—Fiber laser, multi-wavelength, microfiber knot, high nonlinearity.**

I. Introduction

Since the first mode-locked fiber laser was demonstrated in 1986 [1], as a group of highly versatile light sources they have attracted significant due to their ability to access many scientific research fields such as optical communications, sensing, material processing, medical treatment and chemical engineering etc. To date, the two main methods utilized in the operation of pulsed fiber lasers are based on actively mode-locked and passively mode-locked techniques. The passively mode-locked technique is more stable and is an all-fiber solution. In recent years, passively mode-locked techniques have developed rapidly. A large number of passively mode-locked techniques exist and include "the nonlinear optical loop mirror" (NOLM) [2-4], "nonlinear polarization rotation" (NPR) [5-7] and two-dimensional materials [8-24]. The rapid development of passively mode-locked techniques has also provided a foundation for research on multi-wavelength fiber lasers. As an important member of the fiber laser family, the multi-wavelength fiber laser has played a significant role in application areas including dense wave division multiplexing (DWDM), laser distance ranging, spectral analysis, distributed fiber-optic sensing etc. [2]. In recent years an increasing number of two-dimensional materials such as graphene [8-11], topological insulators [12-14], transition metal dichalcogenides [15-22] and black phosphorus [23, 24] have facilitated further advancements in mode-locked lasing research. It has been demonstrated that Graphene can be used in a multi-wavelength fiber laser and this showed that 2D (two-dimensional) materials can be used in the preparation of the saturable absorber (SA) devices to generate a pulsed lasing signal [8]. Topological insulators, sulfide materials, and black phosphorus have also been used in this rapidly developing fiber laser field. Among the two-dimensional materials, few-layer tungsten disulfide (WS_2) which can exist in the form of atomically thin sheets, has allowed the realization of femtosecond pulses in mode-locked fiber lasers which indicates that WS_2 has the necessary

The work was supported by the National Natural Science Foundation of China (NSFC) under grant 61575050; National Key R&D Program of China under grant 2016YFE0126500; Key Program for Natural Science Foundation of Heilongjiang Province of China under grant ZD2016012; the Open Fund of the State Key Laboratory on Integrated Optoelectronics (Grant no: IOSKL2016KF03), this work was also supported by the 111 project (B13015) to the Harbin Engineering University. (Corresponding author: Pengfei Wang)

Shi Li, Yating Yi, Yu Yin, Yuxuan Jiang, Haiyan Zhao, Yanqiu Du, Yujin Chen and Pengfei Wang are with the Key Laboratory of In-fiber Integrated Optics of Ministry of Education, College of Science, Harbin Engineering University, Harbin 150001, China.(e-mail: m18204313488@163.com , rabbit1995icy@hrbeu.edu.cn , cbyy@hrbeu.edu.cn , merak@hrbeu.edu.cn , zhy_physics@163.com , yanqiudu@126.com , chenyujin@hrbeu.edu.cn , pwang@hrbeu.edu.cn)

Elfed Lewis is with Optical Fibre Sensors Research Centre, Department of Electronic and Computer Engineering, University of Limerick, Limerick, Ireland. (e-mail: elfed.lewis@ul.ie)

Gerald Farrell is with Photonics Research Centre, Dublin Institute of Technology, Kevin Street Dublin 8 Ireland. (e-mail: gerald.farrell@dit.ie)

S. W. Harun is with the Department of Electrical Engineering, University of Malaya, 50603 Kuala Lumpur, Malaysia. (e-mail: swharun@um.edu.my)

Pengfei Wang is also with Key Laboratory of Optoelectronic Devices and Systems of Ministry of Education and Guangdong Province, College of Optoelectronic Engineering, Shenzhen University, Shenzhen, 518060, China (e-mail: pengfei.wang@dit.ie).

This article has been accepted for publication in a future issue of this journal, but has not been fully edited. Content may change prior to final publication. Citation information: DOI 10.1109/JLT.2018.2877583, Journal of Lightwave Technology

saturated absorption properties for generation of the pulsed laser [17]. However, researchers have also established that WS_2 materials have a third-order nonlinearity: an excellent quality for the generation of multi-wavelength peaks [15]. Based on this feature, a double-wavelength pulsed laser output has been demonstrated [19, 20]. The useful twin properties of WS_2, i.e. saturated absorption coupled with excellent nonlinearity, has attracted significant recent attention in the area of multi-wavelength fiber lasers. Double-wavelength and triple-wavelength emissions have been obtained by transferring the WS_2 onto a tapered fiber or a fiber connector contained within the laser cavity [19]. However, it is hard to achieve further multiplication of the number of wavelengths using these techniques, as they are limited by the degree of non-linearity available in the WS_2 material [15]. The same paper analyses the possible novel use of the microfiber knot structure to affect an enhancement of the nonlinearity of WS_2 in mode locking fiber lasers.

Since the first microfiber cavity laser was demonstrated [25], optical devices based on microfibers have played a major role in many domains including light detection, communications and sensing due to low cost and ease of preparation [25, 26]. Researchers have developed several resonators based on microfiber, such as the loop resonator [27, 28], knot resonator [29-37] and coil resonator [38, 39]. Among the resonators based on a microfiber, the knot resonator has the recognized advantages of ease of fabrication, simple structure, and compact size [29-32]. However, for a fiber laser, the pump power consumption is a significant challenge due to the inherent weak nonlinearity of silica [40]. The microfiber knot can change its size by simply resizing the resonator while continuing to work stably on a refractive index substrate or in a liquid under test [29]. Additionally, it is possible that the microfiber knot has a significant role to play in conjunction with other optical materials due to the effective photon interaction resulting from the strong evanescent amplification of the microfiber knot geometry [41]. A hybrid structure comprising a microfiber knot resonator combined with graphene has been demonstrated by coating the microfiber knot with graphene [32]. The resulting excellent characteristics include high optical non-linearity and rapid response time, which confirm the possibility that a new device based on the microfiber knot can be highly applicable for non-linear optical device, high performance optical fiber sensors, ultrafast modulators etc. [32]. In recent years several researchers have achieved lasing using a microfiber knot owing to its excellent optical characteristics as outlined above [34-37]. The approach adopted in the investigation reported in this article is based on a new WS_2 device in combination with a microfiber structure to achieve a larger number of output wavelengths. Up to seven output wavelength peaks have been achieved in the experimental work presented in this paper.

The resulting novel saturable absorber (SA) device provides saturable absorption combined with high non-linearity within the newly formed laser cavity. A seven-wavelength pulse was obtained by gradually increasing the pump power and rotating the polarization controller. The results of this work confirm that the microfiber knot enhances the nonlinearity of the WS_2 and hence the new SA device has the significant advantage of high non-linearity for use in nonlinear optics. The SA device can be used widely in the multi-wavelength fiber laser field due to the excellent performance of the SA device in providing multiple peaks due to the combined action of saturable absorption ability and the nonlinearity.

II. Experiment

The WS_2 nanosheets were prepared through a liquid-phase exfoliation method [18]. These nanosheets were dispersed in the ethanol solution with a concentration of about 0.1 mg/ml for further usage. Fig. 1(a) shows the Raman spectrum of the WS_2 nanosheets. Two characteristic peaks were observed at wavelengths centred on ~351.6 and ~418.5 cm^{-1}, corresponding to the in-plane (E_{2g}) and out-of-plane (A_{1g}) vibrational modes of WS_2 when irradiated using an Ar laser at 514 nm [15]. The layer of the WS_2 nanosheets was estimated to be 3-5 layers thick, which is in agreement with previous findings [15]. The scanning electron microscopy (SEM) image (Fig. 1(b)) shows that the WS_2 nanosheets have a lateral length of approximately 300 nm. Fig.1 (c) shows the same TEM image of the WS_2 nanosheets.

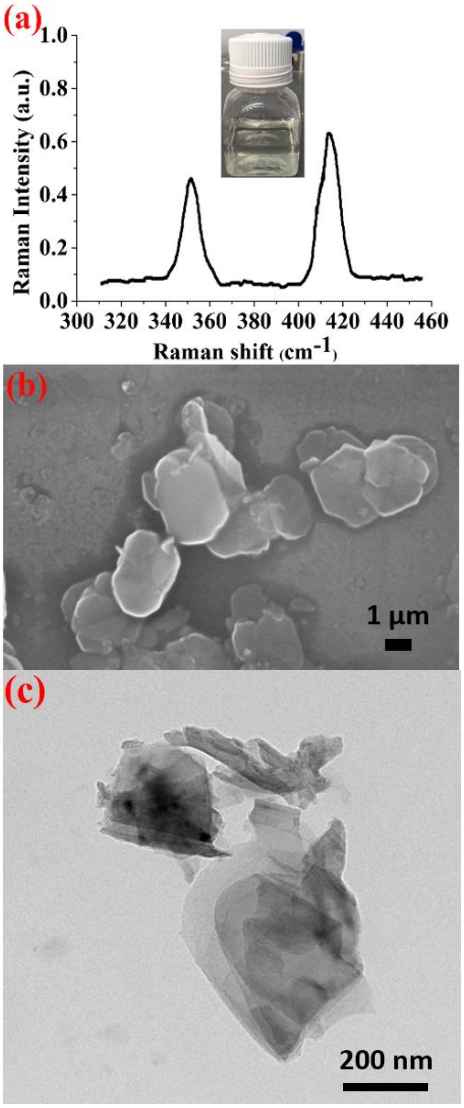

Fig. 1. (a) The Raman spectrum, (b) The SEM image of the WS_2 nanosheets. (c) The TEM image of the WS_2 nanosheets.

The microfiber was prepared using the fused taper method [42] with a tip (waist) diameter of ~ 3 μm which was cleaved at

This article has been accepted for publication in a future issue of this journal, but has not been fully edited. Content may change prior to final publication. Citation information: DOI 10.1109/JLT.2018.2877583, Journal of Lightwave Technology

the transition region at one end and connected to a standard single-mode fiber at the other end. The resulting half tapered microfiber was folded into a knot structure as shown in Fig 2. Initially, the microfiber was cleaved at the transition region and fixed on a 3-axis micro-displacement platform (Newport M-561D-XYZ-LH). Then a short section of single-mode fiber (SMF-28) was used to manipulate the microfiber into a knot structure with the help of electro-static force. The initial microfiber knot diameter was set to be as large with a value of several millimeters to make the subsequent processing steps easier. Another half-tapered microfiber was fixed on a separate 3-axis micro-displacement platform (Newport M-561D-XYZ-RH) and was also brought into contact with the microfiber knot via electrostatic force so that the light from the source can be easily transferred into the structure. Finally, the two micro-displacement platforms were adjusted slightly to control the size of the microfiber knot during experiments. The microfiber knot was formed with a diameter, D ≈ 500 μm as shown photographically in fig. 2(b).

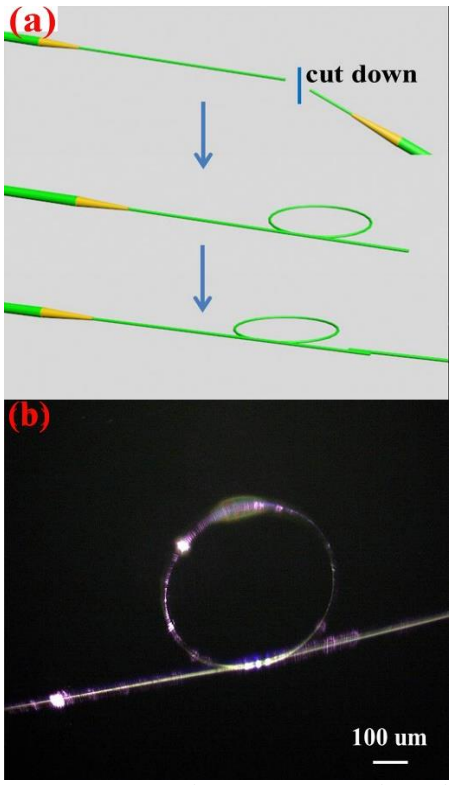

Fig. 2. (a) Schematic illustrations for the construction of microfiber knot. (b) Photograph of the WS_2 device based on the microfiber knot.

To fulfill the role of the WS_2 and the microfiber WS_2 nanosheets were transferred onto the microfiber prepare the WS_2 SA incorporating the knot using the optical deposition method [18]. In this process, light (150 mW) from a 980 nm laser was launched into the microfiber knot while depositing the WS_2 solution onto the structure for more than two hours. Then the SA device was connected to a super continuum source (YSL SC-series) and an OSA (optical spectrum analyzer: YOKOGAWA, AQ-6370C) was used as the detector to measure the transmission spectrum. The experimentally obtained result in Fig. 3(a) shows the full transmission spectrum in the range 1540 to 1560 nm including several optical resonance lines. The absorption line centered on a wavelength of 1542.5 nm is highlighted in Fig 3(a) for which the FSR (free spectral range) is 1.12 nm.

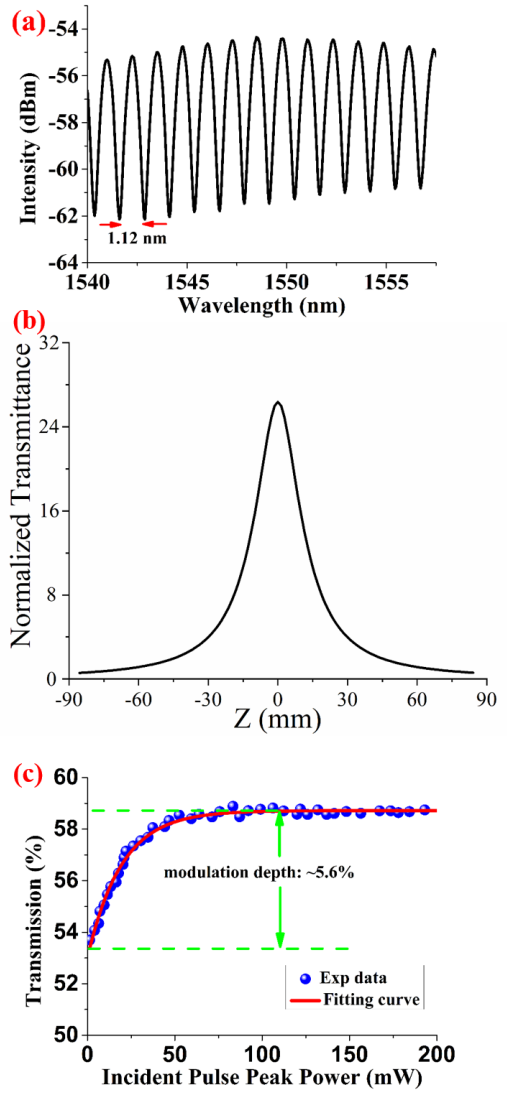

Fig. 3. (a) Transmission spectra of the microfiber knot. (b) A typical z-scan peak curve at 1550 nm. (c) Nonlinear saturable absorption curve.

In order to characterize the third order nonlinearity of the WS_2 device, the z-scan method was used. The results are shown in Fig. 3(b) and clearly indicate that the WS_2 device exhibits nonlinear saturable absorption. As shown in the figure, a typical z-scan peak curve was obtained, confirming that the third order nonlinearity of the WS_2 device exists. The ratio of the maximum to the minimum optical transmittance was as high as 26.5, which was significantly higher than the previously reported device based on graphene [12]. The appearance of such an absorption line is necessary for the pulse generation in the laser and is key for determining whether or not the SA device has the capability for saturable absorption. Fig. 3(c) clearly shows its modulation depth is ~ 5.6%, which was measured using the power-dependent transmission scheme using a femtosecond fiber laser (Center wavelength: 1550 nm, Pulse width: 300 fs, Repetition rate: 15 MHz) as the pump

This article has been accepted for publication in a future issue of this journal, but has not been fully edited. Content may change prior to final publication. Citation information: DOI 10.1109/JLT.2018.2877583, Journal of Lightwave Technology

source [19]. It is clear from this analysis that the SA device has achieved saturable absorption. Finally, the insertion loss of the SA device was measured using an optical power meter. A 1550 nm CW laser was used as the light source to connect with the microfiber knot device incorporating the WS_2 nanosheets at one end, and at the other end the same optical power meter was used to measure the average output power. The output power with and without SA was measured as 12.6 mW, and 25.3 mW, respectively. Therefore, the insertion loss of the SA device was estimated to be about 3 dB.

The experimental setup including the 980 nm pump source (MCPL-980-SM), a 980/1550 nm wavelength division multiplexer (WDM, MCWDM-98/15), a ~5 m length of Erbium-doped fiber (ER16-8/125), a polarization independent isolator (PI-ISO, MCI-1550), a polarization controller (PC, MP-1550), a 10% optical coupler (OC, 1550 FBT Coupler), a section of single mode fiber (SMF 28) and being the key components of the SA device is shown in Fig. 4. The polarization independent isolator (PI-ISO) maintains unidirectional transmission from the laser source preventing potentially damaging back-reflections. 90% of the OC input was maintained within the feedback loop to ensure that adequate laser power was maintained within the fiber laser cavity. The remaining 10% of the OC input was used to couple the circulating signal to the test equipment: an OSA to measure the optical spectrum, an oscilloscope (Tektronix MDO4054-6) to measure the pulse waveform, an optical power meter (Newport 1918-R) to measure the output power, and an autocorrelator (Pulse Check SM 320) to measure the pulse width. A 20 m length of single-mode fiber was incorporated inside the cavity to optimize the dispersion and nonlinear characteristics for mode-locked operation. The total dispersion in the ring laser cavity was calculated to be -1.07 ps^2, which indicates that the laser operates in the anomalous regime.

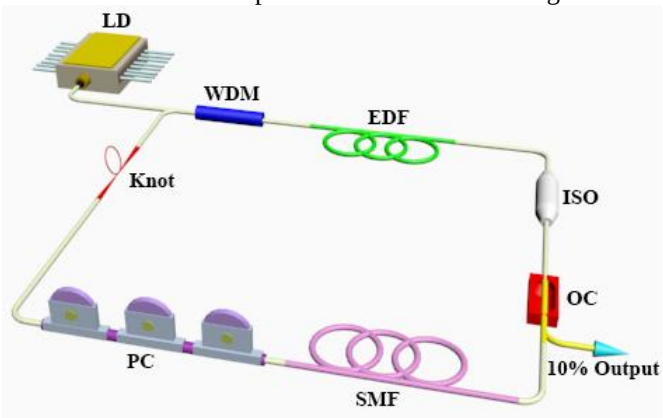

Fig. 4. Schematic of the experimental setup

III. Results and Discussion

Before the SA device was placed into the fiber laser cavity, it was necessary to confirm the working state of the laser to exclude the possibility of NPR (nonlinear polarization rotation) and the occurrence of any Fabry-Perot effect. No mode-locking generation was observed by uprating the pump power from the minimum power output value of 0 to the maximum of 420 mW. This being the case, it is evident that the SA device, when inserted into the cavity, is the sole source of non-linear phenomena for the ring laser.

The SA device was inserted into the laser cavity and the output observed using the OSA and Oscilloscope referred to above. Initially, the pump power was adjusted to ~50 mW, at which value a continuous wave output was clearly observed. The pump power was then gradually increased in the range 86 mW to 350 mW whilst carefully rotating the polarization plane. During this phase it could be determined that multi-wavelength mode-locked operation was achieved. The evolution of the multi-wavelength from initial continuous wave operation clearly indicates that a cavity exists when the laser is working. Generally, if the cavity induced birefringence filter has a large bandwidth, the filtering effect can be ignored [40]. However, the existence of the SA device is a key element of the multi-wavelength pulse generation, which in turn indicates that the SA device based on the microfiber knot plays a key role as wavelength selection to enhance the filtering capability.

In the experiment of this investigation, four-, five-, six-, and seven-wavelength mode-locked outputs have been observed, and the results confirmed that the stable multi-wavelength can be simply achieved from the presence of a nonlinearity introduced by the incorporation of the SA device. Among the numerous phenomena of the multi-wavelength pulse, the seven-wavelength mode-locking pulse was observed when uprating the pump power to ~250 mW. The seven-wavelength optical spectrum is shown in Fig. 5(a). The central wavelength of the 7-wavelength pulse is in the vicinity of 1535 nm and the interval between it and the neighboring wavelength is ~1.02 nm. Each 3dB spectrum bandwidth is ~0.17 nm. Seven flat peaks were observed in Fig. 5 (a), which were most probably due to the power redistribution effect [8] inside the cavity. This effect was caused by the high nonlinearity of the layered WS_2. However, a slight power variation was still observed among the multiple peaks, which was attributed to the gain-spectral characteristic of the EDF [37]. The optimization of the gain spectrum and nonlinear characteristics of the cavity are expected to reduce the power variation further. The typical oscilloscope pulse waveform is shown in Fig. 5(b). The data shows the pulse period to be 188.7 ns, which corresponds to a repetition rate of 5.3 MHz which agrees well with the cavity length of 38.7 m. Some subtle intensity changes were observed in the pulses (amplitude) due to a lower frequency modulation effect. It is clear that the “whispering gallery mode” (WGM) behavior of the microfiber knot can effectively enhance the nonlinearity of the WS_2 to induce multi-wavelength emission. The nonlinearity effect provided by the SA device thus has a stronger role in the mode-locked fiber laser than traditional methods such as those based on tapered fiber [19, 20].

This article has been accepted for publication in a future issue of this journal, but has not been fully edited. Content may change prior to final publication. Citation information: DOI 10.1109/JLT.2018.2877583, Journal of Lightwave Technology

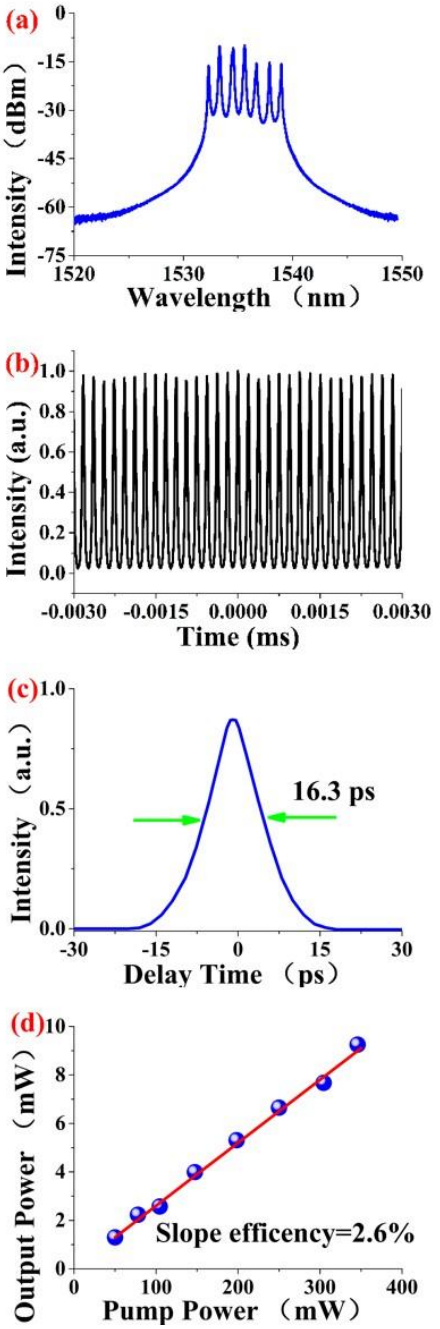

Fig. 5. Seven-wavelength mode-locking characteristics. (a) Optical spectrum. (b) Typical oscilloscope pulse waveform. (c) Autocorrelation trace. (d) Output power versus the pump power

It was possible to filter out one wavelength from the multi-wavelength pulse signal using a bandpass filter, to make sure that the pulse generation in the fiber laser was genuinely due to the multi-wavelength pulse, and hence excluding the influence of "the energy quantization effect" [40]. An autocorrelation trace was measured using an autocorrelator (pulse Check SM 320), for a delay time of 16.3 ps resulted, as shown in the Fig. 5(c). In the experiment, the output power of the fiber laser increased with increasing the pump power. The maximum value of the output power was observed to be 9.1 mW and the linear relationship of the output power and the pump power is clearly shown in Fig. 5(d). Fig. 6 shows the long-term spectrum measured at repeated 2-hour intervals over a 12-hour period. The results clearly show that the fiber laser has excellent long-time stability. The general characteristics of the 7-wavlength pulse and the 12 h spectral time evolution performance are shown in Fig. 5 (a) and Fig. 6 respectively, confirming that the SA device not only shows its saturable absorption stability, but also has a significant non-linear effect with long term stability. Compared with common dual-wavelength and triple-wavelength versions based on the WS_2 tapered fiber and fiber connector, the fiber laser in this investigation exhibits a seven-wavelength pulse, and hence it can be determined that the microfiber knot is the key in the enhancement of the cavity nonlinearity. To verify the effect of the microfiber knot on the nonlinearity in the fiber laser cavity, a further experiment was conducted which is described below.

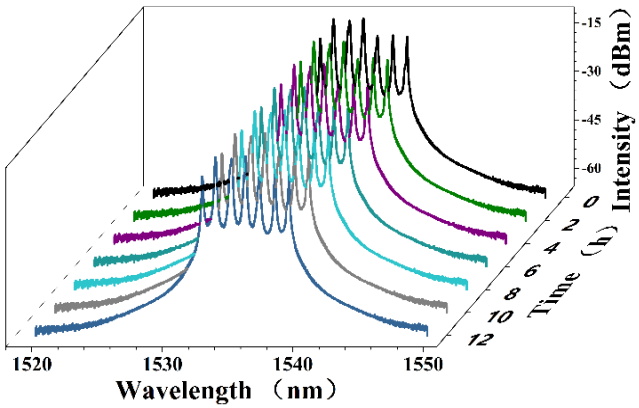

Fig. 6. Long term spectral variation measured at a 2-h interval over 12 hours

A completely new microfiber knot with a diameter D ≈ 750 μm was fabricated; the tapered fiber diameter was ~ 3 μm as previously described. The few-layer WS_2 was transferred onto the microfiber knot using the same optical deposition method as previously used, forming a new WS_2 device based on a revised microfiber knot.

After completing the above steps, the WS_2-deposited microfiber knot was placed into the ring cavity laser. A six-wavelength mode-locked pulse was observed (not seven-wavelengths as in the previous case) at a 250 mW pump power and the spectrum is shown in Fig. 7(a). Compared with the optical spectrum when D is ~ 500 nm, the number of wavelength peaks is one less, but the interval between each peak and the 3-dB spectrum bandwidth remain the same. The corresponding temporal variation for the mode-locked pulse was recorded on an oscilloscope as previously described, and is shown in Fig. 7(b). The pulse waveform is similar to the case for the microfiber knot diameter being 500 μm.

This article has been accepted for publication in a future issue of this journal, but has not been fully edited. Content may change prior to final publication. Citation information: DOI 10.1109/JLT.2018.2877583, Journal of Lightwave Technology

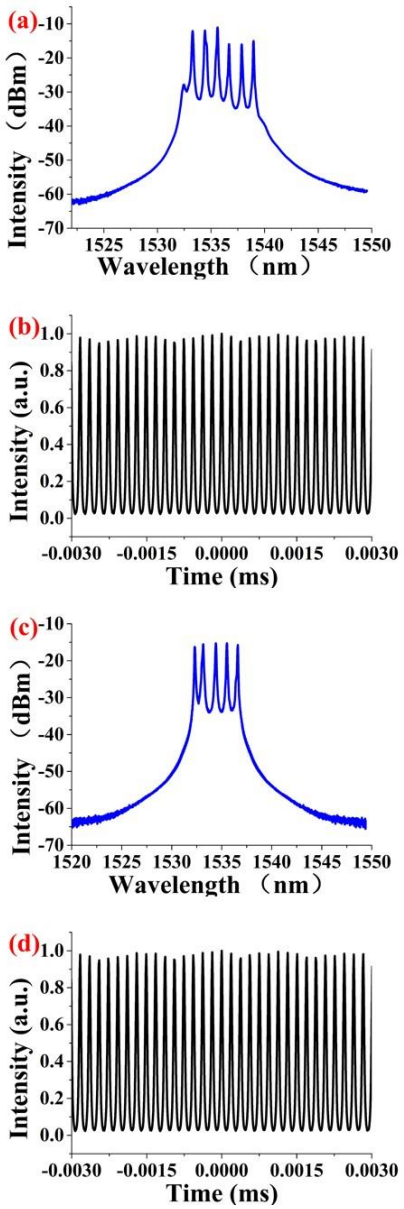

Fig. 7. (a) Six-wavelength mode-locking optical spectrum when the diameter D ≈ 750 μm. (b) Typical oscilloscope pulse waveform when the diameter D ≈ 750 μm. (c) Five-wavelength mode-locking optical spectrum when the diameter D ≈ 1 m., (d) Typical oscilloscope pulse waveform when the diameter D ≈ 1 mm.

The six-wavelength mode-locked pulse was achieved by simply increasing the knot size from 500 μm to 750 μm. The non-linearity in the cavity formed in this case is lower than the previous value (the 500 μm case) because the WGM becomes weaker with the knot diameter increasing [41], and therefore it does not enhance the non-linearity as strongly as in the 500μm case.

Finally, a microfiber knot with the diameter D ≈ 1 mm was also fabricated in the identical manner to the above and this formed a new SA device which was inserted between the WDM and PC as previously described. A Five-wavelength mode-locking pulse was observed and this is shown in Fig. 7(c). Fig. 7(d) shows that the pulse waveform is similar to the case of six and seven-wavelength pulse cases.

Seven-wavelength, six-wavelength and five-wavelength mode-locking peaks have been generated with relative ease by simply varying the knot size; the multi-wavelength number reduces when the nonlinearity effect weakens as the knot diameter is increased. The series of experiments confirms our hypothesis: the microfiber knot enhances the nonlinearity of the WS_2 material but in doing so does not degrade the saturable absorption in a typical microfiber structure.

IV. Conclusion

The experiment confirmed that the dual properties of the SA device have been successfully implemented in a single, novel device and experimentally verified. The WS_2-deposited microfiber knot has a dual role in the emission process: saturable absorption for pulse generation and high-nonlinearity for multi-wavelength generation. In the experiment, a multi-wavelength pulse performance has been achieved by changing the state of the laser. Seven wavelength-operation has been completely described including observing the time resolved pulse waveforms thus allowing measurement of the pulse period and the repetition rate. A major achievement of the work of this investigation has been to establish that the SA device plays a key dual role in the novel laser cavity based device. In addition, six-wavelength and five-wavelength pulse emissions were achieved simply by increasing the knot size. Experiments in which the knot diameter was increased also confirm that the degree of nonlinearity can be varied simply by resizing the knot. Therefore, the novel SA device described in this investigation can be deployed in any field which requires the presence of nonlinear optical phenomena. The inherent advantageous characteristics of excellent saturable absorption and high nonlinearity have resulted in a SA device that can be fabricated with relative ease and readily used as a multi-wavelength fiber laser source, which can in turn be applied in many industrial application scenarios including high density wavelength distributed multiplexing, laser ranging, spectral analysis as well as distributed fiber-optic sensing.

References

[1] U. Keller, "Recent developments in compact ultrafast lasers," Nature 424, 831-838 (2003).

[2] D. U. Noske, M. J. Guy, K. Rottwitt, R. Kashyap, and J. R. Taylor, "Dual-wavelength operation of a passively mode-locked “figure-of-eight” ytterbium-erbium fibre soliton laser," Optics Communications 108, 297-301 (1994).

[3] L. Yun, X. Liu, and D. Mao, "Observation of dual-wavelength dissipative solitons in a figure-eight erbium-doped fiber laser," Optics Express 20, 20992 (2012).

[4] Q. Y. Ning, S. K. Wang, A. P. Luo, Z. B. Lin, Z. C. Luo, and W. C. Xu, "Bright–Dark Pulse Pair in a Figure-Eight Dispersion-Managed Passively Mode-Locked Fiber Laser," IEEE Photonics Journal 4, 1647-1652 (2012).

[5] V. J. Matsas, and T. P. Newson, "Selfstarting passively mode-locked fibre ring soliton laser exploiting nonlinear polarisation rotation," Optics Communications 28, 1391-1393 (1992).

[6] Z. Chen, H. Sun, S. Ma, and N. K. Dutta, "Dual-Wavelength Mode-Locked Erbium-Doped Fiber Ring Laser Using Highly Nonlinear Fiber," IEEE Photonics Technology Letters 20, 2066-2068 (2008).

[7] Z. C. Luo, A. P. Luo, W. C. Xu, H. S. Yin, J. R. Liu, Q. Ye, and Z. J. Fang, "Tunable Multiwavelength Passively Mode-Locked Fiber Ring Laser Using Intracavity Birefringence-Induced Comb Filter," IEEE Photonics Journal 2, 571-577 (2010).

[8] Z. Luo, M. Zhou, Z. Cai, C. Ye, J. Weng, G. Huang, and H. Xu, "Graphene-Assisted Multiwavelength Erbium-Doped Fiber Ring Laser," IEEE Photonics Technology Letters 23, 501-503 (2011).

[9] N. Zhao, M. Liu, H. Liu, X. W. Zheng, Q. Y. Ning, A. P. Luo, Z. C. Luo, and W. C. Xu, "Dual-wavelength rectangular pulse Yb-doped fiber laser using a microfiber-based graphene saturable absorber," Optics Express 22, 10906-10913 (2014).

[10] H. Li, J. Zhao, P. Yan, R. Lin, S. Huang, and Y. Wang, "Tunable and switchable multi-wavelength dissipative soliton generation in a graphene oxide mode-locked Yb-doped fiber laser," Optics Express 22, 11417-11426 (2014).

[11] A. Luo, B. Guan, J. Zhou, X. Feng, X. Wang, and Z. Luo, "Dual-wavelength single-longitudinal-mode fiber laser with switchable wavelength spacing based on a graphene saturable absorber," Photonics Research 3, A21-A24 (2015).

[12] C. Zhao, H. Zhang, X. Qi, Y. Chen, Z. Wang, S. Wen, and D. Tang, "Ultra-short pulse generation by a topological insulator based saturable absorber," Applied Physics Letters 101, 118 (2012).

[13] C. Zhao, D. Tang, H. Zhang, S. Wen, S. Lu, Y. Zou, Y. Chen, and Z. Wang, "Wavelength-tunable picosecond soliton fiber laser with Topological Insulator: Bi_2Se_3 as a mode locker," Optics Express 20, 27888 (2012).

[14] A. P. Luo, C. J. Zhao, H. Zhang, H. Liu, M. Liu, N. Zhao, W. C. Xu, X. W. Zheng, Y. Chen, and Z. C. Luo, "Microfiber-Based Highly Nonlinear Topological Insulator Photonic Device for the Formation of Versatile Multi-Soliton Patterns in a Fiber Laser," Journal of Lightwave Technology 33, 2056-2061 (2015).

[15] A. Berkdemir, H. R. Gutiérrez, A. R. Botello-Méndez, N. Perea-López, A. L. Elías, C.-I. Chia, B. Wang, V. H. Crespi, F. López-Urías, and J.-C. Charlier, "Identification of individual and few layers of WS_2 using Raman Spectroscopy," Scientific reports, vol. 3, p. 1755, 2013.

[16] B. Chen, X. Zhang, K. Wu, H. Wang, J. Wang, and J. Chen, "Q-switched fiber laser based on transition metal dichalcogenides MoS(2), MoSe(2), WS(2), and WSe(2)," Optics Express 23, 26723-26737 (2015).

[17] R. Khazaeinezhad, S. H. Kassani, H. Jeong, K. J. Park, B. Y. Kim, D. I. Yeom, and K. Oh, "Ultrafast Pulsed All-Fiber Laser Based on Tapered Fiber Enclosed by Few-Layer WS_2 Nanosheets," IEEE Photonics Technology Letters 27, 1581-1584 (2015).

[18] M. Dong, Y. Wang, C. Ma, H. Lei, B. Jiang, X. Gan, S. Hua, W. Zhang, T. Mei, and J. Zhao, "WS_2 mode-locked ultrafast fiber laser," Sci Rep 5, 7965 (2015).

[19] B. Guo, Y. Yao, P. G. Yan, K. Xu, J. J. Liu, S. G. Wang, and Y. Li, "Dual-Wavelength Soliton Mode-Locked Fiber Laser With a WS_2-Based Fiber Taper," IEEE Photonics Technology Letters 28, 323-326 (2016).

[20] B. Guo, S. Li, Y. Fan, and P. Wang, "Versatile soliton emission from a WS_2 mode-locked fiber laser," Optics Communications (2017).

[21] P. Yan, A. Liu, Y. Chen, H. Chen, S. Ruan, C. Guo, S. Chen, I. L. Li, H. Yang, and J. Hu, "Microfiber-based WS_2-film saturable absorber for ultra-fast photonics," Optical Materials Express 5, 479 (2015).

[22] P. Yan, A. Liu, Y. Chen, J. Z. Wang, S. Ruan, H. Chen, and J. Ding, "Passively mode-locked fiber laser by a cell-type WS_2 nanosheets saturable absorber," Scientific Reports 5, 12587 (2015).

[23] A. P. Luo, C. J. Zhao, H. Zhang, M. Liu, W. C. Xu, X. F. Jiang, X. F. Yu, Z. C. Luo, and Z. N. Guo, "Microfiber-based few-layer black phosphorus saturable absorber for ultra-fast fiber laser," Optics Express 23, 20030 (2015).

[24] J. Sotor, G. Sobon, M. Kowalczyk, W. Macherzynski, P. Paletko, and K. M. Abramski, "Ultrafast thulium-doped fiber laser mode locked with black phosphorus," Optics Letters 40, 3885-3888 (2015).

[25] K. Vahala, Optical Microcavities (WORLD SCIENTIFIC, 2004).

[26] L. Tong, F. Zi, X. Guo, and J. Lou, "Optical microfibers and nanofibers: A tutorial," Optics Communications 285, 4641-4647 (2012).

[27] M. Sumetsky, Y. Dulashko, J. M. Fini, and A. Hale, "Optical microfiber loop resonator," Applied Physics Letters 86, 816 (2005).

[28] M. Sumetsky, Y. Dulashko, J. M. Fini, A. Hale, and D. J. Digiovanni, "The microfiber loop resonator: theory, experiment, and application," Journal of Lightwave Technology 24, 242-250 (2006).

[29] X. Jiang, L. Tong, G. Vienne, X. Guo, A. Tsao, Q. Yang, and D. Yang, "Demonstration of optical microfiber knot resonators," Applied Physics Letters 88, 1380 (2006).

[30] Z. Chen, V. K. S. Hsiao, X. Li, Z. Li, J. Yu, and J. Zhang, "Optically tunable microfiber-knot resonator," Optics Express 19, 14217-14222 (2011).

[31] K. S. Lim, S. W. Harun, S. S. A. Damanhuri, A. A. Jasim, C. K. Tio, and H. Ahmad, "Current sensor based on microfiber knot resonator," Sensors & Actuators A Physical 167, 60-62 (2011).

[32] Y. Wang, X. Gan, C. Zhao, L. Fang, D. Mao, Y. Xu, F. Zhang, T. Xi, L. Ren, and J. Zhao, "All-optical control of microfiber resonator by graphene's photothermal effect," Applied Physics Letters 108, 922-924 (2016).

[33] X. Jiang, Q. Yang, G. Vienne, Y. Li, L. Tong, J. Zhang, and L. Hu, "Demonstration of microfiber knot laser," Applied Physics Letters 89, 839 (2006).

[34] A. Sulaiman, S. W. Harun, H. Arof, and H. Ahmad, "Compact and Tunable Erbium-Doped Fiber Laser With Microfiber Mach–Zehnder Interferometer," IEEE Journal of Quantum Electronics 48, 1165-1168 (2012).

[35] A. Sulaiman, S. W. Harun, F. Ahmad, S. F. Norizan, and H. Ahmad, "Electrically Tunable Microfiber Knot Resonator Based Erbium-Doped Fiber Laser," IEEE Journal of Quantum Electronics 48, 443-446 (2012).

[36] Y. Xu, L. Ren, C. Ma, X. Kong, and K. Ren, "Demonstration of a stable and uniform single-wavelength erbium-doped fiber laser based on microfiber knot resonator," Optical Engineering 55, 126111 (2016).

[37] M. Liu, H. Liu, X. W. Zheng, and N. Zhao, "Demonstration of Multiwavelength Erbium-Doped Fiber Laser Based on a Microfiber Knot Resonator," IEEE Photonics Technology Letters 26, 1387-1390 (2014).

[38] F. Xu, P. Horak, and G. Brambilla, "Optical microfiber coil resonator refractometric sensor," Optics Express 15, 7888 (2007).

[39] F. Xu, and G. Brambilla, "Demonstration of a refractometric sensor based on optical microfiber coil resonator," Applied Physics Letters 92, 5742 (2008).

[40] Agrawal, and Govind, Nonlinear Fiber Optics (Fifth Edition) (2013).

[41] L. Tong, and M. Sumetsky, Subwavelength and Nanometer Diameter Optical Fibers (Springer-Verlag, 2009).

[42] L. Shi, X. Chen, H. Liu, Y. Chen, Z. Ye, W. Liao, and Y. Xia, "Fabrication of submicron-diameter silica fibers using electric strip heater," Optics Express 14, 5055-5060 (2006).